Chitosan-Modified d-α-Tocopheryl Poly(ethylene glycol) 1000 Succinate-b-Poly(ε-caprolactone-ran-glycolide) Nanoparticles for the Oral Chemotherapy of Bladder Cancer

Baichuan Liu,[1†] Han Wang,[2†] Lixin Fan,[1] Xiaofu Qiu,[1] Youhua Luo,[1] Shenyang Zhou,[1] Guosheng Yang[1]

[1]Department of Urology, Guangdong Number 2 Provincial People's Hospital, Guangzhou, Number 1 Shiliugang Road, Guangzhou, 510317, China
[2]Graduate School of Guangxi Medical University, Nanning, 530021, China
†B. Liu and H. Wang contributed equally to this work..
Correspondence to: G. Yang (E-mail: mlaa002@163.com and 2008yangguosheng@sina.com)

ABSTRACT: Oral chemotherapy is quickly emerging as an appealing option for cancer patients. It is less stressful because the patient has fewer hospital visits and can still maintain a close relationship with health care professionals. Three kinds of nanoparticles made from commercial poly(ε-caprolactone) (PCL) and self-synthesized d-α-tocopheryl poly(ethylene glycol) 1000 succinate -b-poly(ε-caprolactone-ran-glycolide) [TPGS-b-(PCL-ran-PGA)] diblock copolymer were prepared in this study for the oral delivery of antitumor agents, including chitosan-modified PCL nanoparticles, nonmodified TPGS-b-(PCL-ran-PGA) nanoparticles, and chitosan-modified TPGS-b-(PCL-ran-PGA) nanoparticles. First, the TPGS-b-(PCL-ran-PGA) diblock copolymer was synthesized and structurally characterized. Chitosan was adopted to extend the retention time at the cell surface and thus increase the chance of nanoparticle uptake by the gastrointestinal mucosa and improve the absorption of drugs after oral administration. The resulting TPGS-b-(PCL-ran-PGA) nanoparticles were found to be of spherical shape and around 200 nm in diameter with a narrow size distribution. The surface charge of the TPGS-b-(PCL-ran-PGA) nanoparticles could be reversed from anionic to cationic after surface modification. The chitosan-modified TPGS-b-(PCL-ran-PGA) nanoparticles displayed a significantly higher level of cellular uptake compared with the chitosan-modified PCL nanoparticles and nonmodified TPGS-b-(PCL-ran-PGA) nanoparticles. *In vitro* cell viability studies showed the advantages of the chitosan-modified TPGS-b-(PCL-ran-PGA) nanoparticles over Taxol in terms of their cytotoxicity against human RT112 cells. In summary, the oral delivery of antitumor agents by chitosan-modified TPGS-b-(PCL-ran-PGA) nanoparticles produced results that were promising for the treatment of patients with bladder cancer. © 2013 Wiley Periodicals, Inc. J. Appl. Polym. Sci. 130: 2118–2126, 2013

INTRODUCTION

Bladder cancer remains one of the most commonly diagnosed cancers worldwide. Oral chemotherapy is assuming an increasingly important role in bladder cancer therapy. The main advantage of the oral delivery of anticancer drugs is the convenience; the patient can receive chemotherapy at home without having to go to the hospital and sit through a couple of hours of intravenous infusions. Another great benefit to the oral delivery of anticancer drugs is that it gives the patient more control over his or her own cancer care.[1] However, most antitumor agents, especially those with excellent anticancer effects such as paclitaxel (PTX), are poorly absorbed in the gastrointestinal (GI) tract. This is because the oral administration of PTX shows

an extremely poor oral bioavailability (<1%).[2–4] A P-glycoprotein (P-gp) pump in the mucosa of the GI tract may limit the absorption of the orally administered PTX and mediate their direct excretion into the lumen of the small intestine.[4,5] First-pass metabolism by cytochrome P450 isoenzymes in the intestinal wall and/or the liver may also contribute to the poor oral bioavailability of PTX.[4,6] Alternative treatment approaches to enhance the oral bioavailability of PTX and other antitumor agents are currently under intense investigation.[2,7,8] The general treatment approach is to make use of P-gp and cytochrome P450 3A4 inhibitors such as cyclosporine A to suppress the elimination process; however, this also weaken the body's immune system and thus creates severe complications during

cancer treatment.[4,8] Nanoparticles of biodegradable polymers are highly attractive from the pharmaceutical point of view because of their desirable properties, including biodegradability, biocompatibility, and controlled release. Furthermore, such nanoparticles could prevent recognition by the P-gp efflux pump and thus have the strong potential to improve the oral bioavailability of poorly absorbed or presystemically metabolized drugs.[4,9–11] Because of their small size, the nanoparticles have a very high specific surface area and dispersion; this can promote their absorption compared to larger drug carriers. In addition, nanoparticles of biodegradable polymers may shield their encapsulated contents from luminal degradation and intestinal metabolism.[4,7] Moreover, they could reduce or inhibit the multidrug resistance (MDR) that characterizes many antitumor agents by a mechanism of the cellular internalization of the drug and reduce or inhibit its efflux from cells mediated by the P-gp.

It seems to be a commonly accepted notion in the world today that the particle surface properties are very important for their uptake by intestinal epithelial cells. Therefore, alternative methodologies and innovative techniques have been adopted to enhance the intestinal absorption of nanoparticles, either by modification of their surface properties or by the conjugation of targeting molecules at their surface.[12] It is thought that the presence of a cationic surface charge promotes the interaction and binding of nanoparticles to the endosomal membrane and induces membrane destabilization and cytosolic relocalization of the nanoparticles.[7,13–15] The cationic charge of chitosan derivatives caused by the primary amino groups in theirs structure is believed to be liable for their mucoadhesive properties and, therefore, extends the residence time at the absorption site.[16,17] Thus, chitosan-modified nanoparticles are expected to become appropriate carriers for promoting oral drug absorption.[16,18] Chitosan derivatives have lots of advantages as drug carriers in nanoparticle-based delivery systems. They are considered to be biodegradable, nontoxic, and biocompatible. In addition, they have been also proven to control the release of drugs, proteins, and peptides. They are soluble in aqueous solutions, prevent the use of organic solvents, and do not require the further purification of nanoparticles.[18,19] Thus, chitosan derivatives were used in this study to be absorbed on the nanoparticle surface by the nature of ionic interactions between cationic and anionic.

In this research, poly(ε-caprolactone) (PCL)-ran-polyglycolide (PGA) was used to retain the desirable mechanical strength of the copolymer. Vitamin E d-α-tocopheryl poly(ethylene glycol) 1000 succinate (TPGS) is a water-soluble derivative of naturally sourced vitamin E. Structurally, it has a dual nature with hydrophilicity and lipophilicity, similar to a surfactant. It was reported that TPGS was capable of improving drug transport through various biological membranes by the inhibition of P-gp efflux pumps and thus enhanced the extent of absorption for poorly soluble drugs and reduced the P-gp-mediated MDR of resistant tumor cells.[20–22] In addition, TPGS was capable of effectively suppressing the growth of cancer cells in animal and cell culture models.[23] The main reasons for the superior antitumor activity of TPGS is its increasing ability to induce apoptosis in tumor cell lines.[23–25] Previous studies have shown synergistic effects of combinations of vitamin E isomers or derivatives such as TPGS with other antitumor agents.[24] In addition, it has been reported that TPGS-emulsified nanoparticles had a higher encapsulation efficacy, longer half-life, and better therapeutic efficiency of the formulated drug than those emulsified by poly(vinyl alcohol), a commonly used emulsifier in nanoparticle formulation process.[22] Thus, we were inspired to fabricate a novel chitosan-modified TPGS-b-(PCL-ran-PGA) nanoparticle as oral anticancer drug carrier for bladder cancer chemotherapy. The chemical structure of TPGS-b-(PCL-ran-PGA) is shown in Figure 1.[26]

EXPERIMENTAL

Materials

TPGS [$C_{33}O_5H_{54}(CH_2CH_2O)_{23}$] and chitosan were acquired from Sigma-Aldrich (St. Louis, MO). TPGS-b-(PCL-ran-PGA) copolymer (weight-average molecular weight = 25,000 Da) and PTX powder with a purity of 99.9% were obtained from NanoMed Biotech Co., Ltd. (Shenzhen, China). PCL (molecular weight = 42,000 Da) and stannous octoate [$Sn(OOCC_7H_{15})_2$] were also purchased from Sigma-Aldrich. Fetal bovine serum was received from Gibco (Life Technologies, AG, Switzerland). Methanol and acetonitrile were acquired from EM Science (Mallinckrodt Baker). Deionized (DI) water produced by Millipore Water Systems was used throughout all of the experiments.

Characterization of the TPGS-b-(PCL-ran-PGA) Copolymer

The TPGS content and number-average molecular weight (M_n) of the copolymer was measured by ^{1}H-NMR in CDCl$_3$ at 300 Hz (Bruker ACF300). The weight-average molecular weight and molecular weight distribution were detected by gel permeation chromatography (Waters gel permeation chromatography analysis system, Milford).

Preparation of the Chitosan-Modified PTX-Loaded Nanoparticles

Nanoparticles were prepared by a modified solvent extraction/evaporation technique.[27–29] In brief, 11 mg of PTX powder and 100 mg of TPGS-b-(PCL-ran-PGA) copolymer were weighed and dissolved in 6 mL of methylene chloride. The organic solution was immediately poured into 100 mL of a 0.03% w/v TPGS solution under mild stirring. The mixture was then sonicated for 90 s at a 30-W output to form a water-in-oil emulsion. The water-in-oil emulsion was evaporated further under ambient conditions overnight to remove residual methylene chloride. The nanoparticles were harvested by centrifugation at 80,000 × g for 20 min and then washed three times to remove the unencapsulated drug and emulsifiers. The resulting nanoparticles were finally resuspended in 5 mL of DI water and lyophilized. The TPGS-b-(PCL-ran-PGA) nanoparticles were further modified by chitosan with a previously described protocol.[13] Preweighed chitosan was dissolved in DI water at a concentration of 0.5 mg/mL. The nanoparticles were suspended in a chitosan solution at a concentration of 9.5 mg/mL by sonication at a 30-W power output for 30 s over an ice bath and were then collected by centrifugation at 80,000 × g for 20 min. The coumarin 6 (C6)-loaded nanoparticles were fabricated by the encapsulation of 0.1% w/v C6 instead of PTX. The chitosan-modified PCL nanoparticles were fabricated by the same method.
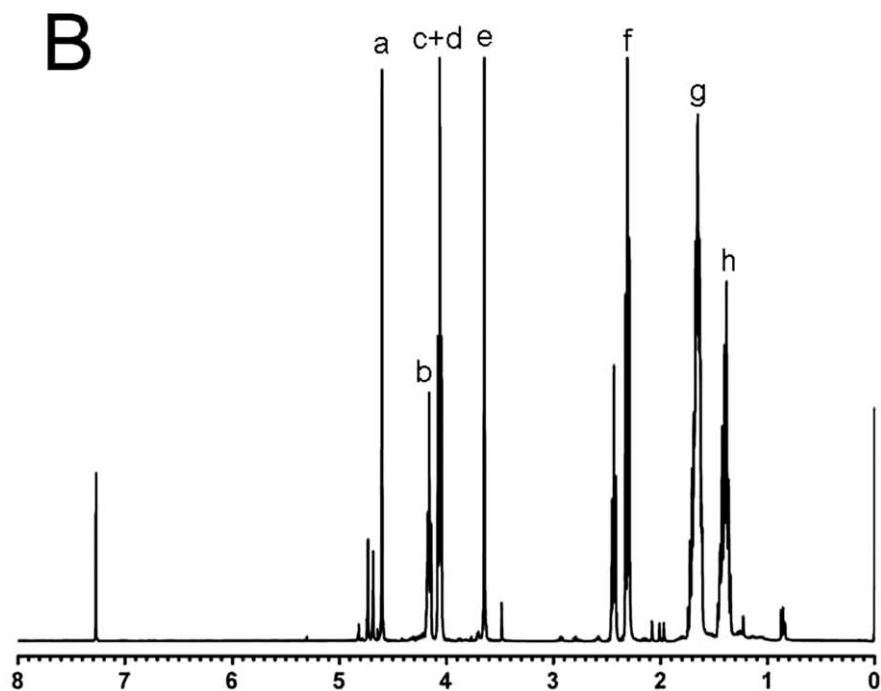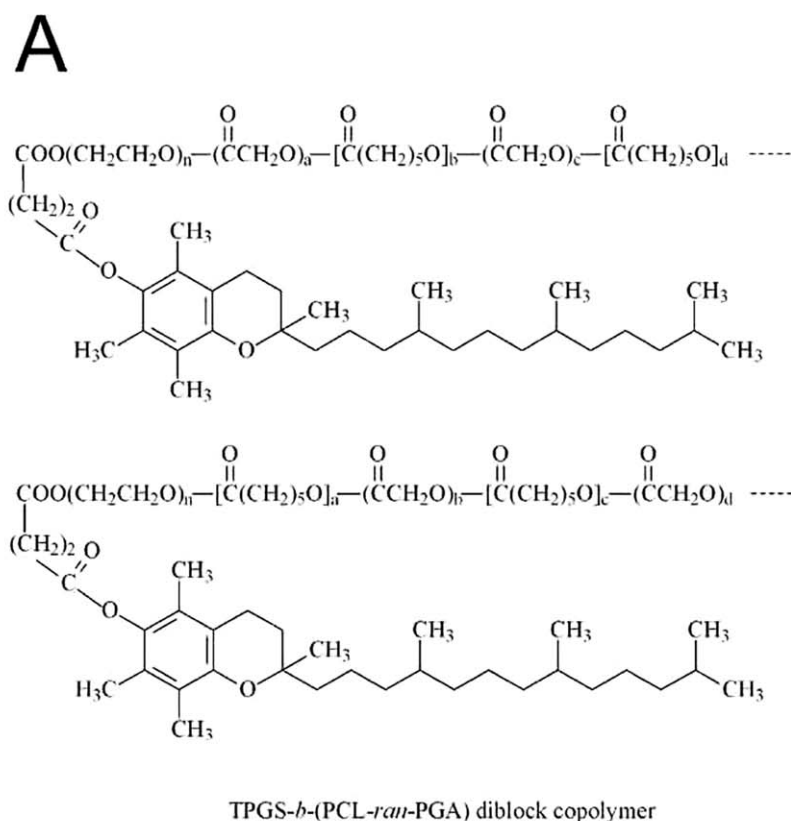
Figure 1. (A) Chemical structure of the TPGS-*b*-(PCL-*ran*-PGA) copolymer and (B) typical ^{1}H—NMR spectra of the TPGS-*b*-(PCL-*ran*-PGA) copolymer.

Nanoparticle Characterization

Particle Size and ζ Potential. The mean particle diameter and range of the particle size distribution were detected with dynamic light scattering on a Malvern Zetasizer Nano-ZS90 (Malvern Instruments, Worcestershire, United Kingdom). The lyophilized nanoparticles were diluted with DI water before measurement. The surface charge of the nanoparticles was determined by laser–Doppler anemometry with a Zetasizer

Nano Series instrument (Malvern Instruments). All measurements were performed in triplicate.

Morphology of the Nanoparticles. The morphology of the nanoparticles was examined by field emission scanning electron microscopy (FE-SEM; Zeiss 77 SUPRA 40VP) at a 5.0-kV electron high tension. To prepare samples for FE-SEM observations, a drop of the diluted aqueous suspension of the nanoparticles was placed on 400-mesh, carbon-coated copper grid, and the supernatant liquid was removed with a capillary after the particles were allowed to settle. The particles were then coated with platinum layer for 30 s.

Drug Loading and Encapsulation Efficiency. The entrapment efficiency (EE; %) and the drug-loading capacity of the nanoparticles was determined by high-performance liquid chromatography (HPLC; LC 1200, Agilent Technologies, Santa Clara, CA) as described previously.[13,30] In short, dried nanoparticles (5 mg) were dissolved in 1 mL of methylene chloride under vigorous vortexing. The organic solution was transferred to 5 mL of a mobile phase consisting of acetonitrile and DI water (50:50 v/v). Methylene chloride was evaporated under a stream of nitrogen gas until a clear solution was obtained. The samples were then used for HPLC analysis. The column effluent was monitored at 227 nm with an ultraviolet–visible detector. The standard size HPLC column (4.6 × 250 mm) was run at a flow rate of 1 mL/min. The drug EE was defined as the percentage of the drug loaded in the final product. All of these experiments were performed in triplicate.

***In Vitro* Drug-Release Assay.** Accurately weighted aliquots of the drug-loaded nanoparticles (15 mg) were suspended in 5 mL of release medium (PBS at pH 7.4 containing 0.1% w/v Tween 80). The use of Tween 80 in the release medium made it possible to enhance the solubility of the lipophilic drugs in the aqueous solution and prevent the binding of drug to the tube wall. The nanoparticle suspension was transferred into a dialysis tubing membrane, which was sealed at one end with a clamp. The sealed dialysis bag was placed into a centrifuge tube and immersed in 15 mL of release medium. The centrifuge tube was put into an orbital water bath shaking at 130 rpm at 37.0°C. Aliquots of the samples (10 mL) were periodically aspirated for HPLC analysis and replaced with fresh medium. The collected samples were extracted with 2 mL of methylene chloride and reconstituted in 5 mL of the mobile phase. Methylene chloride was evaporated under a stream of nitrogen gas until a clear solution was obtained. The analysis procedure was the same as that used for the determination of the drug EE.

Cellular Uptake of the Polymeric Nanoparticles
Caco-2 cells, which were acquired from the American Type Culture Collection (Manassas, VA), were used in this study to simulate the GI barrier for oral chemotherapy. The cells were grown in tissue culture flasks maintained at 37°C in a humidified 5% CO_2 atmosphere. The medium, Dulbecco's modified essential medium (DMEM) supplemented with 100 μg/mL of streptomycin and 20% fetal bovine serum, was freshened once every 3 days. After 70–90% confluence was reached, the cells were harvested with a 0.25% trypsin–ethylene diamine tetraacetic acid solution (Invitrogen) and cultured in a 96-well black plate (Corning, Inc., Corning, NY) at a density of 1.3×10^4 cells per well. When the cells reached confluence, the cells were equilibrated with Hank's balanced salt solution (HBSS) buffer at 37°C for 60 min and then incubated with the C6-loaded nanoparticle suspension medium. The nanoparticles were well-dispersed in the cell culture medium at concentrations of 100, 250, and 500 μg/mL. The nanoparticle dispersions were incubated in a 5% CO_2-humidified atmosphere for 2 h at 37°C. After incubation with the corresponding nanoparticles, the suspension was removed from the wells, and the cell monolayers were rinsed three times with 50 μL of cold PBS (pH 7.4) to remove residual nanoparticles left in the wells. After that, the cells were lysed with 50 μL of 0.5% w/v Triton-X 100 in a 0.2N NaOH solution. The fluorescence intensity present in each well was then determined on a GENios Lueifcrase microplate reader (TECAN, Switzerland) with an excitation wavelength of 430 nm and an emission wavelength of 485 nm. The cellular uptake efficiency was expressed as the percentage of cells associated fluorescence of that present in the positive control. The culturing of human bladder cancer cell lines RT112 cells and their uptake of the C6-loaded nanoparticles were performed with the same protocol.

Caco-2 cells were reseeded in a Lab-Tek chambered cover glass system (Nalge Nunc International, Rochester, NY). After the cells were incubated with a 250 μg/mL C6-loaded chitosan-modified TPGS-*b*-(PCL-*ran*-PGA) particle suspension at 37°C for 2 h, the cells were rinsed with cold PBS three times and then fixed with a 70% ethanol solution for 20 min. The cells were then rinsed twice with a PBS solution and then counterstained with 4′,6-diamidino-2-phenylindole dihydrochloride (DAPI; Fluka, Buche, Switzerland) for visualization of the cell nuclei. The cell monolayer was rinsed twice with the PBS solution and mounted with the Dako fluorescent mounting medium (Dako, Carpinteria, CA) to be observed by confocal laser scanning microscopy (CLSM; Olympus Fluoview FV-1000, Tokyo, Japan). The images of the cells were determined with a differential interference contrast channel, and the images of the C6-loaded nanoparticles and the nuclei of the cells stained by DAPI were recorded with the following channels: green channel (C6) with excitation at 488 nm and blue channel (DAPI) with excitation at 340 nm.

Cell Viability Assay
The RT112 cells were counted and seeded in 96-well plates at a density of 0.5×10^4 cells per well and incubated overnight to allow cell attachment. The cells were incubated with a drug-loaded TPGS-*b*-(PCL-*ran*-PGA) nanoparticle suspension; chitosan-modified TPGS-*b*-(PCL-*ran*-PGA) nanoparticles; Taxol at 0.25, 2.5, 12.5, and 25 μg/mL equivalent PTX concentrations; and blank chitosan-modified TPGS-*b*-(PCL-*ran*-PGA) nanoparticles with the same amount of nanoparticles for 24, 48, and 72 h, respectively. At predetermined time intervals, the nanoparticles were replaced with fresh DMEM containing 3-(4,5-dimethyl-2-thiazolyl)-2,5-diphenyl-2H-tetrazolium bromide (MTT) (5 mg/mL), and the cells were then incubated for an additional 4 h. The MTT-containing medium was aspirated off, and 150 mL of DMSO was added to dissolve the formazan crystals formed by living cells. The absorbance of each group was measured by a microplate reader (model 680, Bio-Rad

Table I. Effects of Chitosan Modification on the Size, Encapsulation Efficiency, and ζ Potential

Group	Polymer	Size (nm)	PDI	ζ potential (mV)	Drug content (%)	EE (%)	Chitosan modification (%)
CPNPs	PCL	233.52 ± 4.58	0.243	-17.23 ± 4.13	8.53	85.22	5
UNPs	TPGS-*b*-(PCL-*ran*-PGA)	225.29 ± 2.19	0.158	-20.16 ± 3.16	9.68	96.72	None
CTNPs	TPGS-*b*-(PCL-*ran*-PGA)	246.17 ± 2.34	0.191	23.17 ± 3.14	9.44	94.26	5
DNP	TPGS-*b*-(PCL-*ran*-PGA)	249.35 ± 4.26	0.238	26.18 ± 5.02	9.06	90.55	20

PDI, polydispersity index. $n = 3$.

Laboratories, United Kingdom) at wavelength of 570 nm. The optical density of formazan formed in the control (untreated) cells was taken as 100% viability, and the cells without addition of MTT were used as blanks to calibrate the spectrophotometer to zero absorbance. The value of the concentration required to reduce the cell viability by 50% as compared to the control cells (IC_{50}) for each sample was calculated by the curve fitting of the cell viability data. The results are expressed as the mean plus or minus the standard deviation of one representative experiment done in triplicate, and the experiments were done three times.

Statistical Analyses
The data are expressed as the mean plus or minus the standard deviation. A student's *t* test was used to detect the significance between the means of the variables. A *p* value of less than 0.05 was considered to indicate a statistically significant difference.

RESULTS AND DISCUSSION
Characterization of the Copolymer and Polymeric Nanoparticles
Characterization of the TPGS-*b*-(PCL-*ran*-PGA) Copolymer. In an attempt to confirm the formation of the TPGS-*b*-(PCL-*ran*-PGA) copolymer, an ^{1}H-NMR spectrum measurement was conducted, and the data are shown in Figure 1(B). The peaks at 1.40 (h), 1.66 (g), 2.30–2.43 (f), and 4.08 ppm (d) were due to methylene protons in the PCL units.[26] The characteristic absorption at 3.66 ppm [Figure 1(B), peak e] belonged to the —CH_2 protons of the poly(ethylene oxide) (PEO) part of TPGS. The small peaks in the aliphatic zone were attributed to various moieties of the vitamin E tails.[26] It was reasonable that two kinds of copolymers would be obtained because of the difference between the two peaks at 4.06 (peak c) and 4.16 ppm (peak b; Figure 1). In addition, it can be suggested that both the CL and GA monomers copolymerized with the TPGS monomers from the appearance of the two different peaks. The characteristic absorption peak at 4.63–4.82 ppm (peak a) existed and belonged to the methylene (CH_2) protons of the PGA units. M_n of the TPGS-*b*-(PCL-*ran*-PGA) copolymer was calculated with the ratio between the peak areas at 4.06, 4.63–4.82, and 3.66 ppm. M_n of the TPGS-*b*-(PCL-*ran*-PGA) copolymer detected by ^{1}H-NMR was 23,852. Furthermore, M_n of the TPGS-*b*-(PCL-*ran*-PGA) copolymer detected by gel permeation chromatography was 25,811; this was almost the same as that detected by ^{1}H-NMR. The polydispersity index of the copolymer molecular weight was low and was around 1.27.

Size, ζ Potential, and Encapsulation Efficiency. The particle size and size distribution data of the 5% chitosan-modified poly(ε-caprolactone) nanoparticles (CPNPs), nonmodified TPGS-*b*-(PCL-*ran*-PGA) nanoparticles (UNPs), 5% chitosan-modified TPGS-*b*-(PCL-*ran*-PGA) nanoparticles (CTNPs), and 20% chitosan-modified TPGS-*b*-(PCL-*ran*-PGA) nanoparticles (DNP) fabricated in this research are presented in Table I. The particle size was considered to be an important parameter with regard to particle uptake. The submicrometer particle size may have provided a relatively large surface area and an increase in mucosal absorption; this resulted in high mucoadhesive properties and ability for the nanoparticles.[18] The permeability of the nanoparticles through the intestinal mucosa decreased with increasing nanoparticle size and reached a cutoff diameter around 500 nm.[31,32] The resulting particles were found to be 220–260 nm; this was in the size range in favor of the intestinal absorption of the nanoaprticles.[2,7] The results also reveal that the addition of chitosan led to a slight increase in the particle size. ζ potential measurements were conducted to confirm that the surface modification with 5% chitosan reversed the TPGS-*b*-(PCL-*ran*-PGA) nanoparticles from a negative surface charge of -20.16 mV to a significantly positive charge of 23.17 mV. As suggested in literature, a positive surface charge could enhance the mucosal absorption of the nanoparticles because of anionic nature of the mucous layer.[33]

With regard to the drug EE, we found from Table I that the cationic nanoparticles in the CTNP group achieved the entrapment of PTX with a higher efficiency than the nanoparticles in the CPNP group. This might have been due to the self-emulsification properties of the TPGS segment in the TPGS-*b*-(PCL-*ran*-PGA) copolymer.[2,7]

Surface Morphology. The morphology of the CTNPs was determined by FE-SEM. Figure 2 displays the typical FE-SEM images of the CTNPs. The FE-SEM image further confirmed the particle size determined by laser light scattering. The chitosan-modified nanoparticles displayed well-formed spherical shapes with a random rough surface.

***In Vitro* Release Assay.** The *in vitro* PTX release profiles of the UNPs, CPNPs, and CTNPS are presented in Figure 3. The accumulation PTX release for all three nanoparticle formulations basically started with a burst effect of release followed by a slow release or a release approaching zero. The PTX releases from the CTNPs were believed to be 32.96 and 55.65% of the entrapped drug in the first 5 and 28 days, respectively; this was much faster
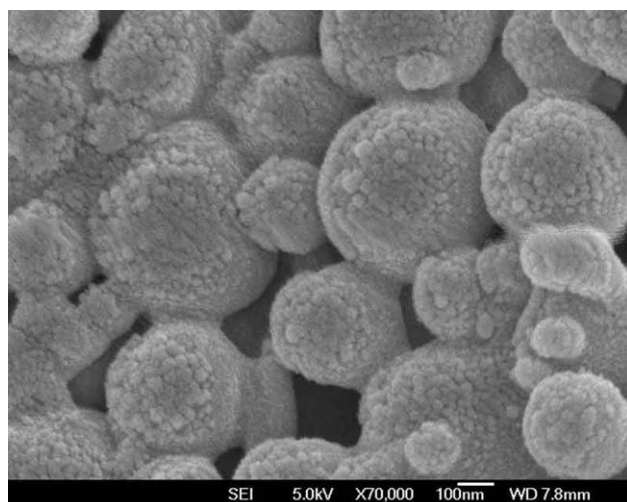
Figure 2. FE-SEM image of the PTX-loaded CTNPs.

Figure 3. *In vitro* release profile of the PTX-loaded CPNPs, UNPs, and CTNPs. [Color figure can be viewed in the online issue, which is available at wileyonlinelibrary.com.]

than those from the CPNPs, which were only 17.10 and 31.58%, respectively, within the same time periods. The faster PTX release of the CTNPs might have been due to the higher hydrophilicity and lower molecular weight of the TPGS-*b*-(PCL-*ran*-PGA) copolymer compared with the PCL nanoparticles. The hydrophilic monomeric units in the TPGS-*b*-(PCL-*ran*-PGA) may have caused the copolymer to swell and degrade much faster; this accelerated the PTX release from the matrix. Figure 3 also showed that the PTX release from the CTNPs was slightly slower than that of the UNPs. This phenomenon may have been due to the slightly smaller nanoparticle size of the UNPs.

Cellular Uptake Studies

The Caco-2 colonic cell line is a well-established and generally accepted model to predict drug absorption and permeability in drug discovery.[34] PTX has been proven to be effective against metastatic bladder cancer as a single drug and in combination with other antitumor agents. The fluorescence uptake by the RT112 cells was capable of providing a useful model for evaluation of the *in vitro* growth inhibition effect of PTX in various pharmaceutical formulations for bladder cancer therapy.[35,36]
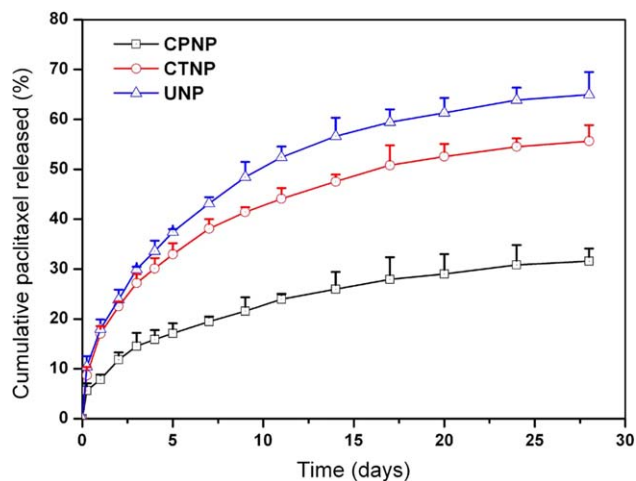
The cellular uptake of the C6-loaded CPNPs, UNPs and CTNPs was thus assessed in this study with Caco-2 cells as an *in vitro* model for the GI barrier and RT112 cells as a model for bladder cancers. The cellular uptake efficiencies of the fluorescence nanoparticles by both Caco-2 and RT112 cells were detected after 2 h of incubation, and the results are presented in Figure 4.

As shown in Figure 4(A), there was an increasing trend in the Caco-2 cellular uptake in which CTNPs > CPNPs > UNPs. The cellular uptake of the CTNP group was up to 1.49-, 1.61-, and 1.70-fold higher than that of the CPNP group and 1.52-, 1.74-, and 1.75-fold higher than that of UNP group at the incubated nanoparticle concentration of 100, 250, and 500 μg/mL, respectively. Figure 4(A) also shows that the cellular uptake was dependent on the particle concentration.

Figure 4(B) shows that the cellular uptake efficiency of the CTNP group by RT112 cells was higher than that of both the CPNP group and UNP group; it was also found to be dose-dependent. The CTNP group resulted in 1.53-, 1.71-, and 1.98-fold higher cellular uptakes than that of CPNP group and 1.34-, 1.38-,
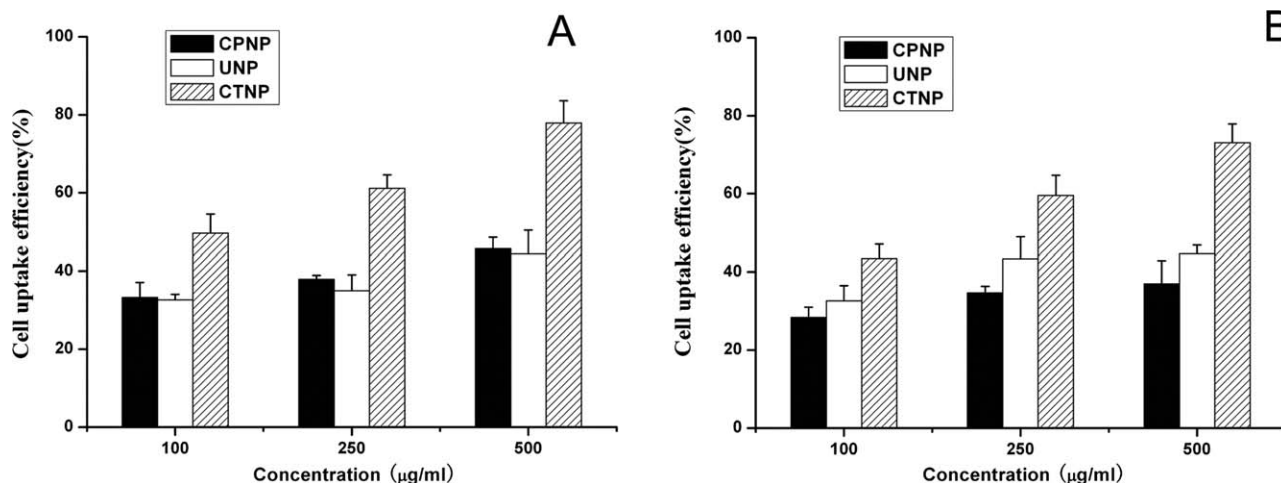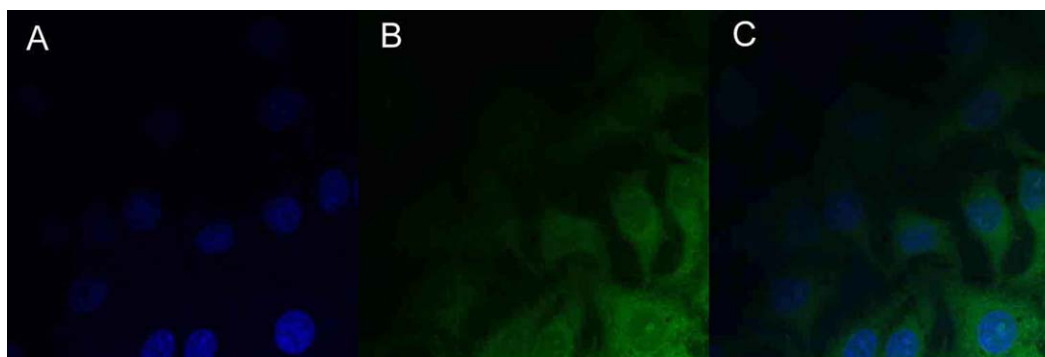

Figure 4. Cellular uptake of the C6-loaded CPNPs, UNPs, and CTNPs by the (A) Caco-2 and (B) RT112 cells after 2 h of incubation.

Figure 5. CLSM images of the Caco-2 cells after 2 h of incubation with the C6-loaded CTNPs at 37.0°C. The cells were stained by DAPI (blue), and the C6-loaded nanoparticles are green. The cellular uptake was visualized by overlaying images obtained by an enhanced green fluorescent protein (EGFP) filter and DAPI filter: (A) DAPI channel, (B) EGFP channel, and (C) combined EGFP channel and DAPI channel. [Color figure can be viewed in the online issue, which is available at wileyonlinelibrary.com.]

and 1.64-fold higher cellular uptakes than that of the UNP group at incubated nanoparticle concentrations of 100, 250, and 500 μg/mL, respectively. The cellular uptake efficiency of the nanoparticles depended mainly on the surface characteristics of the nanoparticles. The positively charged surface of the chitosan derivatives offers a big incentive for aiding drug adsorption and delivery because it is considered to ensure better interaction with the negatively charged cell membrane.[13,15] This would result in extended retention time at the cell surface and thus increase the chances of nanoparticle uptake by the GI mucosa and improve the absorption of drugs after oral administration.[37]

Figure 5 displays a series of CLSM images of the Caco-2 cells after 2 h of incubation with the C6-loaded CTNPs at a nanoparticle concentration of 250 μg/mL. The images were acquired from the green fluorescent protein (green) channel, the DAPI (blue) channel, and the overlay of the two channels. As shown in Figure 5, the fluorescence of the C6-loaded CTNPs (green) was localized predominantly to the cytoplasm surrounding the nucleus (stained by DAPI); this indicated that the cationic nanoparticles were internalized into the cultured Caco-2 cells by endocytosis.[38]
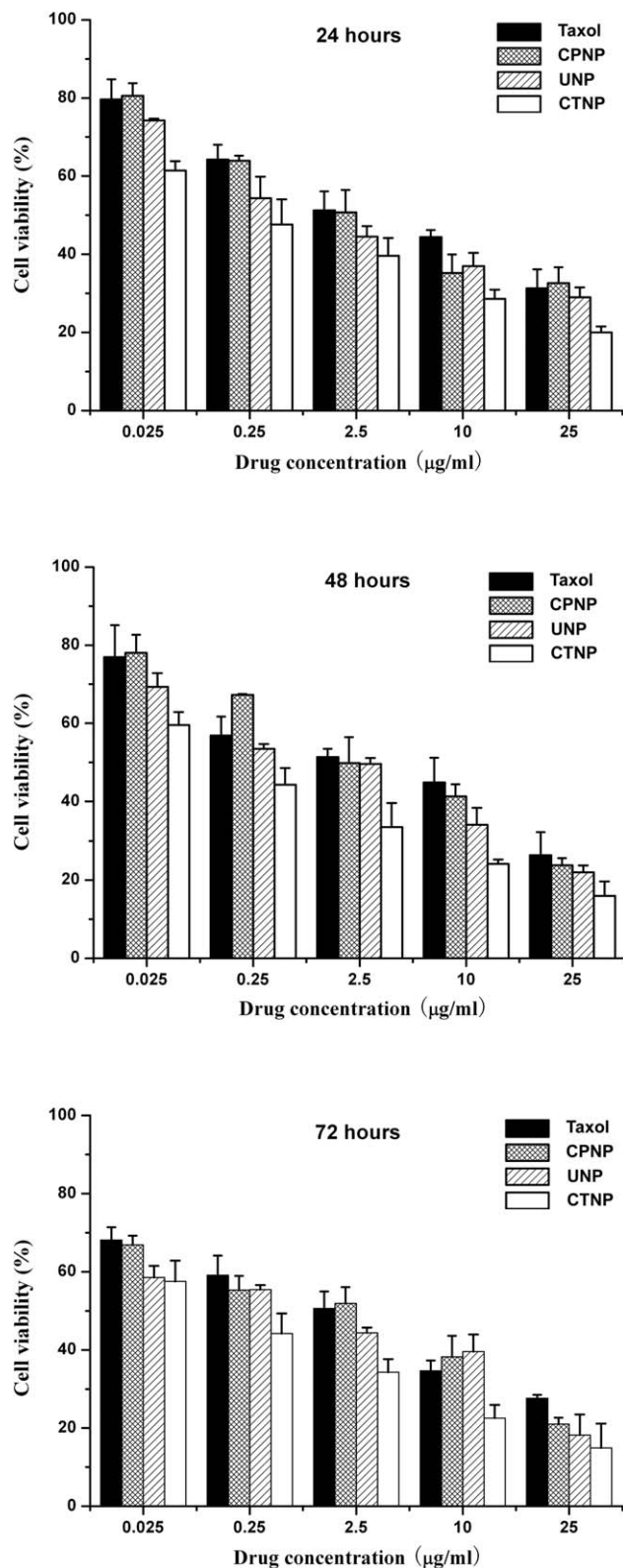
Assessment of the Cationic Nanoparticle Cytotoxicity

Figure 6 shows the viability of the RT112 bladder cancer cells after incubation for 24, 48, and 72 h with PTX formulated in the CPNPs, UNPs, and CTNPs, respectively, compared with those of the current clinical dosage form Taxol at the same 0.025, 0.25, 2.5, 10, and 25 μg/mL PTX doses. It can be summarized from Figure 6 that all three nanoparticles provided advantages in reducing the cell viability of the bladder cancer cells versus commercial Taxol and the CTNPs could have even better therapeutic effects than the UNPs. For example, the cell viabilities of the RT112 cancer cells after 24 h of incubation at the 10 μg/mL drug concentration were 44.39% for Taxol and 28.63% for the CTNPs (i.e., a there was a 28.37% increase in cytotoxicity). In addition, in comparison with Taxol, the cytotoxicities of the RT112 cells were increased by 37.61% ($p < 0.05$, $n = 6$) and 18.62% ($p < 0.05$, $n = 6$) for the CTNPs after 48 and 72 h of incubation at the 10 μg/mL drug concentration. This

might have been due to the synergistic effects of the chitosan and TPGS component of the polymeric nanoparticles in increasing the cellular uptake of the nanoparticles. The results also show that the advantages in cancer cell viability of the groups (CTNP group > UNP group > Taxol formulation) were found to be dependent on the incubation time. This might have been due to the sustained or controlled release manner of the nanoparticles. Furthermore, the advantages in the cancer cell viability of the groups (CTNP group > UNP group > Taxol formulation) were also found to be dependent on the drug concentration.

The advantages in the cytotoxicity of the groups (CTNP group > UNP group > Taxol) could be quantitatively analyzed by their IC$_{50}$ values, which could be determined by the construction of a dose–response curve. Table II displays the IC$_{50}$ values of the RT112 cancer cells after 24, 48, and 72 h of incubation with PTX formulated in the CPNPs, UNPs, CTNPs, and Taxol, respectively; these values were acquired from Figure 6. The data shows that the IC$_{50}$ values for the RT112 cells were reduced from 2.608, 1.636, and 0.909 to 0.200, 0.121, and 0.105 μg/mL for CTNP group after 24, 48, and 72 h of incubation, respectively. As time went on, the CTNP group displayed better and better *in vitro* therapeutic effects for the RT112 cancer cells versus the Taxol formulation. This was probably because the cumulative releases of PTX were only 17.97, 23.88, and 29.93% for the CTNPs after 24, 48, and 72 h of incubation (Figure 3), respectively, and the PTX release started from zero, whereas the Taxol immediately became 100% available for the RT112 bladder cancer cells in the culture. Moreover, the degradation of the TPGS-*b*-(PCL-*ran*-PGA) diblock copolymer might have released the TPGS fragments, which had considerable synergistic antitumor activity in combination with antitumor agents[24,25] and thus increased the cancer cell mortality. Hasegawa et al.[39] reported that chitosan and its derivatives had antioxidant and cytotoxic effects on benzidine-induced bladder cancer and the T24 human bladder cancer cell line.[40] They also observed elevated caspase 3 like activity in chitosan-treated cancer cells and DNA fragmentation, which is characteristic of apoptosis. Chitosan and its derivatives were thus believed to induce apoptosis via caspase 3 activation in the bladder tumor cells.[39] Therefore,

Table II. IC$_{50}$ Values of the RT112 Cells After 24, 48, and 72 h of Incubation with PTX Formulated in the Taxol, CPNPs, UNPs, and CTNPs

Incubation time (h)	IC$_{50}$ (μg/mL)			
	CPNPs	UNPs	CTNPs	Taxol
24	2.034	0.957	0.200	2.608
48	1.747	0.633	0.121	1.636
72	0.691	0.324	0.105	0.909

chitosan and its derivatives are also considered to increase cancer cell mortality and have synergistic antitumor activity in combination with antitumor drugs and TPGS.

CONCLUSIONS

Three kinds of nanoparticles were developed from biodegradable self-synthesized TPGS-*b*-(PCL-*ran*-PGA) diblock copolymer and commercial PCL for the oral delivery of antitumor agents with PTX employed as a model drug; these included CPNPs, UNPs, and CTNPs. The nanoparticle matrix material was designed to take full advantage of TPGS in the nanoparticle fabrication process, including its high emulsification effects, high entrapment efficiency, and improvements in the therapeutic effects in bladder cancer cells, such as a reduction of the P-gp-mediated MDR and the induction of apoptosis. Chitosan was adopted to extend the retention time at the cell surface and thus increased the chances of nanoparticle uptake by the GI mucosa and improved the absorption of drugs after oral administration. The results show that the chitosan-modified TPGS-*b*-(PCL-*ran*-PGA) nanoparticles had a significantly higher level of the cell uptake than the chitosan-modified PCL nanoparticles and UNPs. The *in vitro* cell viability studies showed the advantages of the chitosan-modified TPGS-*b*-(PCL-*ran*-PGA) nanoparticles over commercial Taxol in terms of cytotoxicity against the RT112 cells. In short, the oral delivery of antitumor agents by chitosan-modified TPGS-*b*-(PCL-*ran*-PGA) nanoparticles offers an attractive alternative approach to the treatment of bladder cancer.

REFERENCES

1. Choy, H.; Park, C.; Yao, M. *Clin. Cancer Res.* **2008**, *14*, 1633.

2. Feng, S. S.; Mei, L.; Anitha, P.; Gan, C. W.; Zhou, W. *Biomaterials* **2009**, *30*, 3297.

3. Kuppens, I. E.; Bosch, T. M.; van Maanen, M. J.; Rosing, H.; Fitzpatrick, A.; Beijnen, J. H.; Schellens, J. H. *Cancer Chemother. Pharmacol.* **2005**, *55*, 72.

4. Mei, L.; Zhang, Z.; Zhao, L.; Huang, L.; Yang, X. L.; Tang, J.; Feng, S. S. *Adv. Drug Delivery Rev.*, **2013**, doi: 10.1016/j.addr.2012.11.005.

5. Wils, P.; Phung-Ba, V.; Warnery, A.; Lechardeur, D.; Raeissi, S.; Hidalgo, I. J.; Scherman, D. *Biochem. Pharmacol.* **1994**, *48*, 1528.

Figure 6. Cell viability of the RT112 cells after 24 h (upper), 48 h (middle), and 72 h (lower) of treatment with PTX formulated in the CPNPs, UNPs, and CTNPs in comparison with that of Taxol at the same PTX dose (*n* = 6).

6. Marre, F.; Sanderink, G. J.; de Sousa, G.; Gaillard, C.; Martinet, M.; Rahmani, R. *Cancer Res.* **1996**, *56*, 1296.

7. Chen, H. B.; Zheng, Y.; Tian, G.; Tian, Y.; Zeng, X. W.; Liu, G.; Liu, K. X.; Li, L.; Li, Z.; Mei, L.; Huang, L. Q. *Nanoscale Res. Lett.* **2011**, *6*, 4.

8. Ikezoe, T.; Hisatake, Y.; Takeuchi, T.; Ohtsuki, Y.; Yang, Y.; Said, J. W.; Taguchi, H.; Koeffler, H. P. *Cancer Res.* **2004**, *64*, 7426.

9. Pandey, R.; Zahoor, A.; Sharma, S.; Khuller, G. K. *Int. J. Pharm.* **2005**, *301*, 268.

10. Chen, H.; Langer, R. *Adv. Drug Delivery Rev.* **1998**, *34*, 339.

11. Florence, A. T.; Hussain, N. *Adv. Drug Delivery Rev.* **2001**, *50*(Suppl. 1), S69.

12. des Rieux, A.; Fievez, V.; Garinot, M.; Schneider, Y. J.; Préat, V. *J. Controlled Release* **2006**, *116*, 1.

13. Mei, L.; Sun, H.; Jin, X.; Zhu, D.; Sun, R.; Zhang, M.; Song, C. *Pharm. Res.* **2007**, *24*, 955.

14. Mei, L.; Sun, H.; Song, C. *J. Pharm. Sci.* **2009**, *98*, 2040.

15. Leroueil, P. R.; Hong, S.; Mecke, A.; Baker, J. R., Jr.; Orr, B. G.; Banaszak Holl, M. M. *Acc. Chem. Res.* **2007**, *40*, 335.

16. Saremi, S.; Atyabi, F.; Akhlaghi, S. P.; Ostad, S. N.; Dinarvand, R. *Int. J. Nanomed.* **2011**, *6*, 119.

17. Rudzinski, W. E.; Aminabhavi, T. M. *Int. J. Pharm.* **2010**, *399*, 1.

18. Hosseinzadeh, H.; Atyabi, F.; Dinarvand, R.; Ostad, S. N. *Int. J. Nanomed.* **2012**, *7*, 1851.

19. Agnihotri, S. A.; Mallikarjuna, N. N.; Aminabhavi, T. M. *J. Controlled Release* **2004**, *100*, 5.

20. Zhang, Z.; Mei, L.; Feng, S. S. *Nanomedicine* **2012**, *7*, 1645.

21. Dintaman, J. M.; Silverman, J. A. *Pharm. Res.* **1999**, *16*, 1550.

22. Ma, Y.; Zheng, Y.; Liu, K.; Tian, G.; Tian, Y.; Xu, L.; Yan, F.; Huang, L.; Mei, L. *Nanoscale Res. Lett.* **2010**, *5*, 1161.

23. Youk, H. J.; Lee, E.; Choi, M. K.; Lee, Y. J.; Chung, J. H.; Kim, S. H.; Lee, C. H.; Lim, S. J. *J. Controlled Release* **2005**, *107*, 43.

24. Constantinou, C.; Papas, A.; Constantinou, A. I. *Int. J. Cancer* **2008**, *123*, 739.

25. Neuzil, J.; Tomasetti, M.; Zhao, Y.; Dong, L. F.; Birringer, M.; Wang, X. F.; Low, P.; Wu, K.; Salvatore, B. A.; Ralph, S. J. *Mol. Pharmacol.* **2007**, *71*, 1185.

26. Huang, L. Q.; Chen, H. B.; Zheng, Y.; Song, X. S.; Liu, R. Y.; Liu, K. X.; Zeng, X. W.; Mei, L. *Integr. Biol.* **2011**, *3*, 951.

27. Mei, L.; Zhang, Y.; Zheng, Y.; Tian, G.; Song, C.; Yang, D.; Chen, H.; Sun, H.; Tian, Y.; Liu, K.; Li, Z.; Huang, L. *Nanoscale Res. Lett.* **2009**, *4*, 1530.

28. Gu, H.; Song, C.; Long, D.; Mei, L.; Sun, H. *Polym. Int.* **2007**, *56*, 1272.

29. Ma, Y.; Zheng, Y.; Zeng, X.; Jiang, L.; Chen, H.; Liu, R.; Huang, L.; Mei, L. *Int. J. Nanomed.* **2011**, *6*, 2679.

30. Ma, Y.; Huang, L. Q.; Song, C. X.; Zeng, X. W.; Liu, G.; Mei, L. *Polymer* **2010**, *51*, 5952.

31. Florence, A. T. *Drug Discovery Today* **2005**, *2*, 75.

32. Norris, D. A.; Puri, N.; Sinko, P. *J. Adv. Drug Delivery Rev.* **1998**, *34*, 135.

33. Hariharan, S.; Bhardwaj, V.; Bala, I.; Sitterberg, J.; Bakowsky, U.; Ravi Kumar, M. N. *Pharm. Res.* **2006**, *23*, 184.

34. Artursson, P.; Palm, K.; Luthman, K. *Adv. Drug Delivery Rev.* **2001**, *46*, 27.

35. Nabholtz, J. M.; Tonkin, K.; Smylie, M.; Au, H. J.; Lindsay, M. A.; Mackey, J. *Expert Opin. Pharmacother.* **2000**, *1*, 187.

36. Yan, F.; Zhang, C.; Zheng, Y.; Mei, L.; Tang, L.; Song, C.; Sun, H.; Huang, L. *Nanomedicine: NBM* **2010**, *6*, 170.

37. Bhardwaj, V.; Ankola, D. D.; Gupta, S. C.; Schneider, M.; Lehr, C. M.; Kumar, M. N. *Pharm. Res.* **2009**, *26*, 2495.

38. Zhang, Y.; Tang, L.; Sun, L.; Bao, J.; Song, C.; Huang, L.; Liu, K.; Tian, Y.; Tian, G.; Li, Z.; Sun, H.; Mei, L. *Acta Biomater.* **2010**, *6*, 2045.

39. Hasegawa, M.; Yagi, K.; Iwakawa, S.; Hirai, M. *Jpn. J. Cancer Res.* **2001**, *92*, 459.

40. Kuppusamy, S.; Karuppaiah, J. *Asian Pacific. J. Trop.* **2012**, *2*, S769.